Physica B 177 (1992) 333–338
North-Holland

PHYSICA B

Magnetotransport studies of the organic metals $(BEDT\text{-}TTF)_2AuBr_2$ and $(BEDT\text{-}TTF)_2KHg(SCN)_4$

F.L. Pratt[a], M. Doporto[a], J. Singleton[a], T.J.B.M. Janssen[b], J.A.A.J. Perenboom[b], M. Kurmoo[c], W. Hayes[a] and P. Day[d]

[a]*Clarendon Laboratory, Department of Physics, University of Oxford, Parks Road, Oxford OX1 3PU, UK*
[b]*High Field Magnet Laboratory, NL-6525 ED Nijmegen, The Netherlands*
[c]*Inorganic Chemistry Laboratory, South Parks Road, Oxford, UK*
[d]*Institut Laue-Langevin, BP 156X, Avenue des Martyrs, 38042 Grenoble Cedex, France*

We report magnetoresistance measurements on ET_2 $KHg(SCN)_4$ and $\beta''ET_2$ $AuBr_2$. Both show Shubnikov–de Haas oscillation frequencies additional to those expected from band structure calculations, and other magnetoresistance anomalies occur (e.g. hysteresis, "kink" structures). These effects are explained qualitatively by band structure modifications produced by magnetic ordering.

Charge transfer salts of the ion ET [1] are of great fundamental interest, as they mimic many of the properties of high-T_c superconductors and heavy fermion compounds. The electronic properties of the salts are quasi-two-dimensional, and electron–electron correlation and interaction effects are very important [1]. In this work, we have studied such effects by performing measurements of the magnetoresistance (MR) in the organic metals ET_2 $KHg(SCN)_4$ and $\beta''ET_2$ $AuBr_2$ in fields up to 30 T applied at a variety of orientations and at temperatures between 0.4 and 10 K.

$\beta''ET_2$ $AuBr_2$ and ET_2 $KHg(SCN)_4$ crystals were prepared as described previously [2–4]; the crystals are small black distorted-diamond shaped platelets in form. Both materials have the layer structure typical of a metallic ET salt, resulting in highly conducting planes separated by layers of anions [2–5]. The resistance between the ET layers was measured by attaching gold wires on both sides of the platelets using platinum paint. The MR was studied over a wide range of fields, orientations and temperatures. Calibrated RuO resistance thermometers were used for temperature measurement.

Figure 1(a) shows MR data from $\beta''ET_2$ $AuBr_2$, taken at 490 mK. With the field applied perpendicular to the *ac* plane (see ref. [5] for a definition of the crystal axes), a prominent series of Shubnikov–de Haas oscillations (SdHo)

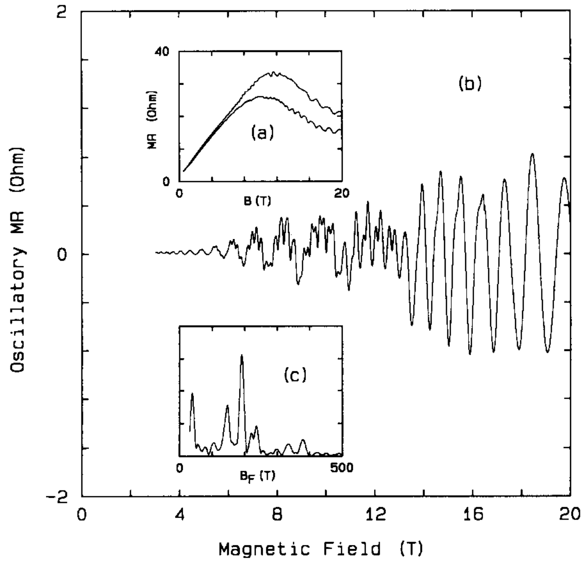

Fig. 1. (a) $\beta''ET_2$ $AuBr_2$ magnetoresistance (MR) at 490 mK for B parallel to $\boldsymbol{b}^*$ (upper trace, 0°) and for B tilted 30° from $\boldsymbol{b}^*$ about $\boldsymbol{a}'$ towards $\boldsymbol{c}$ (lower trace). (b) The oscillatory part of the 30° MR. (c) Fourier spectrum of the 0° trace shown in fig. 1(a).

0921-4526/92/$05.00

can be seen (series I), apparently modulated by a lower frequency. On tilting about the $\boldsymbol{a}'$ direction ($\boldsymbol{a}'$ is perpendicular to both $\boldsymbol{b}^*$ and $\boldsymbol{c}$) to 30° away from the surface normal ($\boldsymbol{b}^*$), the lower frequency becomes visible as a second set of SdHo (series II). With the background MR subtracted (fig. 1(b)), splitting of the SdHo maxima of series I becomes visible in the range 9–14 T, possibly due to the resolution of spin-split Landau levels. A Fourier transform of the MR with the magnetic field perpendicular to the *ac* plane (fig. 1(c)) plainly shows peaks due to SdHo series I ($B_F \simeq 200$ T) and II ($B_F \simeq 40$ T), along with the sums and differences of these two primary frequencies and their harmonics. Hence, series I and II correspond to closed pockets ~2.5% and ~0.5% of the room temperature Brillouin zone (RTBZ) area [2, 5].

Figures 2(a) and (b) show MR data for several tilt angles θ (about $\boldsymbol{a}'$). Note that both series I and II move up in total field approximately as $1/\cos(\theta)$, as expected for a quasi-2D metal, and that the II series grows in prominence as θ increases. Figures 2(c) and (d) show the MR at fixed field as a function of tilt angle for rotation about the $\boldsymbol{a}'$ and $\boldsymbol{c}$ directions, respectively; note the large anisotropy of the MR for rotation about the latter direction. Oscillations are also observed in the MR, corresponding to the conditions derived by Yamaji [6] (fig. 2(d)).

The calculated Fermi surface [5] (fig. 3(a)) has just one closed hole pocket of ~5% of the RTBZ area, together with a pair of open sections aligned along the a' direction; the open areas could give rise to the observed MR anisotropy. Although the closed hole pocket is at first sight a factor of two too large to correspond to SdHo series I, it should be remembered that the curvature of the band leading to the closed pocket is large [6], so that a small adjustment of, e.g.,

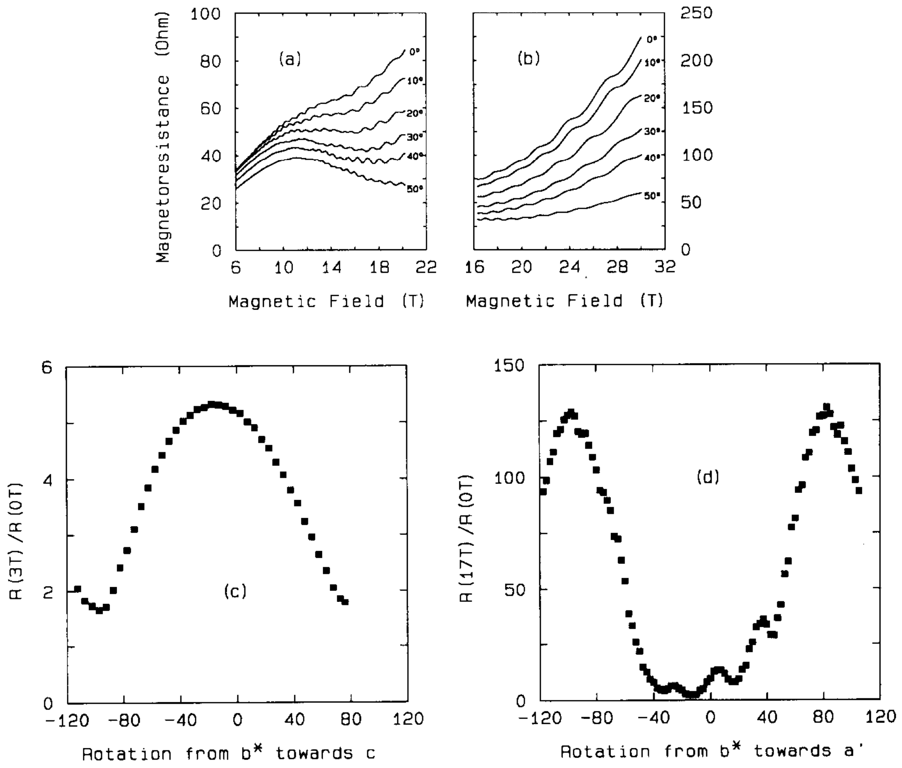

Fig. 2. (a,b) MR as a function of tilt angle about $\boldsymbol{a}'$ ($T = 490$ mK). (c) MR at 3 T for tilting about $\boldsymbol{a}'$ axis ($T = 1.7$ K). (d) MR at 17 T for tilting about $\boldsymbol{c}$ axis ($T = 1.7$ K). In all three cases, the angle θ denotes the angle between B and $\boldsymbol{b}^*$.

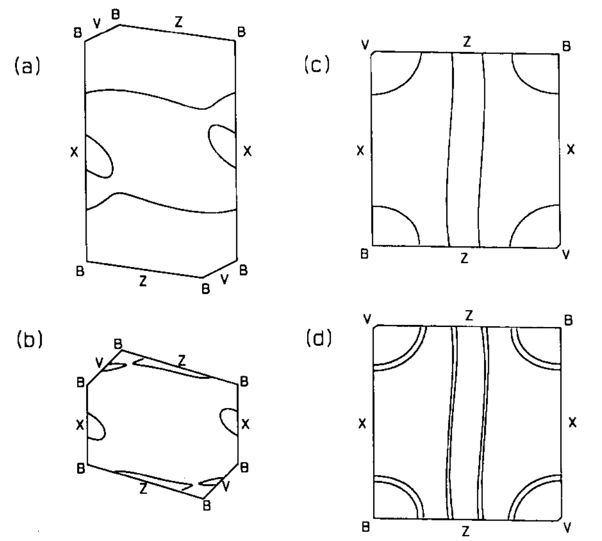

Fig. 3. Calculated Fermi surfaces of $ET_2KHg(SCN)_4$ and $\beta''ET_2AuBr_2$. (a) Fermi surface of $\beta''ET_2AuBr_2$ showing a hole pocket around X and a pair of open sheets. (b) Fermi surface of $\beta''ET_2AuBr_2$ after the formation of a $2c$ SDW. The sheets form a pair of anisotropic closed pockets. (c) Fermi surface of $ET_2KHg(SCN)_4$. The closed hole pocket around B/V is probably associated with the primary SdHo frequency. (d) Fermi surface of $ET_2KHg(SCN)_4$ after inter-layer antiferromagnetic ordering assuming suitable values for the exchange energy and inter-plane bandwidth [7].

the overlaps could result in a large reduction in pocket area. However, the calculated Fermi surface contains no obvious candidate for series II. We therefore propose that the additional SdH frequencies are the result of a $2c$ spin density wave (SDW) modulation driven by the nesting properties of the quasi-one-dimensional open part of the Fermi surface. Evidence for this SDW has been seen in the spin susceptibility below ~20 K [3, 7]. The result of such a SDW modulation is seen in fig. 3(b); a small pocket (hole-like) is produced close to V, along with a very anisotropic closed section of Fermi surface (electron-like) with its long axis approximately parallel to a'; the latter is orientated in the correct sense to be responsible for the MR anisotropy. The band-filling is such that there should be equal number of electrons and holes, so that the total area of the two hole pockets should be the same as the area of the anisotropic electron pocket. In this way, if we identify the two hole pockets with SdHo series I and II, the SdHo due to the electron pocket should occur at the sum of the frequencies of I and II; such a peak is indeed present at $B_F = 240$ T (see fig. 2(c)). As the pocket is so anisotropic, and because the oscillations will overlap with the sum frequency of I and II with some arbitrary phase, we expect the oscillations at $B_F = 240$ T to be weaker than those due to the hole pockets.

Turning to $ET_2KHg(SCN)_4$, fig. 4(a) shows the MR of a sample at 490 mK, and fig. 4(b) the same data with the slowly varying background subtracted. Note that two primary SdH frequencies are present causing beating, and these, their harmonics, sums and differences are plainly visible in the Fourier spectrum of the MR (fig. 4(c)). One of the SdH frequencies, which we shall label $F1$, at $B_F = 667 \pm 3$ T, is present in all samples, whereas the other SdH frequency $F2$ is sample- or cooling-method-dependent, ranging from $\sim F1 + 100$ T to $\sim F1 + 200$ T; in previously

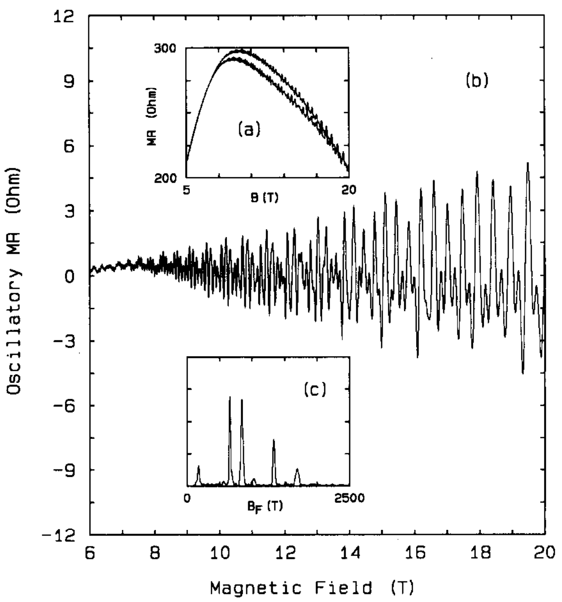

Fig. 4. (a) MR of a sample of $ET_2KHg(SCN)_4$ showing hysteresis; the upper trace is the upsweep, the lower the downsweep. (b) Oscillatory component of MR showing beats and spin-splitting. (c) Fourier spectrum of fig. 4(b) showing two frequencies $F1$ and $F2$ plus their harmonics and frequency mixing.

studied samples [8], $F2$ appears to have been only about 5–10 T higher than $F1$. Note also that there is significant hysteresis between traces recorded on the upsweep of the field and the downsweep (fig. 4(a)), indicating the presence of an effective internal magnetic field; we have found that the degree of hysteresis correlates roughly with the size of the difference between $F1$ and $F2$.

In fig. 5 we show the field dependence of the Fourier amplitudes of $F1$ and $F2$. The points are obtained by transforming within a $0.1\,T^{-1}$ wide data window. Note that as one goes to higher field (lower inverse field), $F2$ falls in amplitude, whereas $F1$ follows the expected Dingle factor dependence.

Figure 6 shows the high-field MR for several angles between the field and the sample surface normal. At angles up to 50°, a large drop of "kink" [8] in resistance occurs around 22 T. Note that above this transition the two series of SdH oscillations become one, with a frequency $B_F = 656 \pm 10$ T (slightly lower than, but within the experimental errors of $F1$), and that the hysteresis between upsweep and downsweep almost vanishes. The SdHo frequency follows a $1/\cos\theta$ dependence as expected for a 2D metal, and there are the SdHo amplitude oscillations expected from the varying spin to cyclotron splitting ratio as the tilt angle increases; analysis [9] of

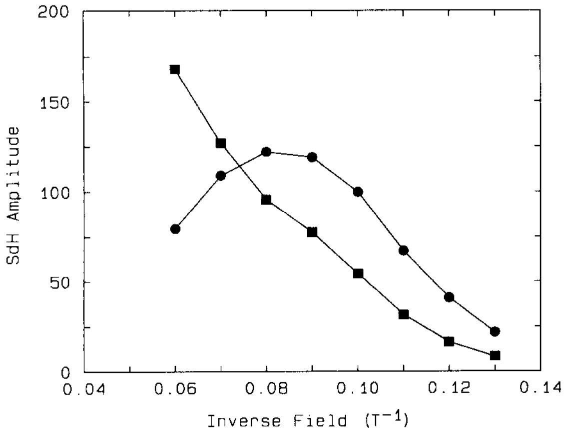

Fig. 5. Fourier amplitudes of $F1$ and $F2$. These points are obtained by transforming within a shifting $0.1\,T^{-1}$ wide data window.

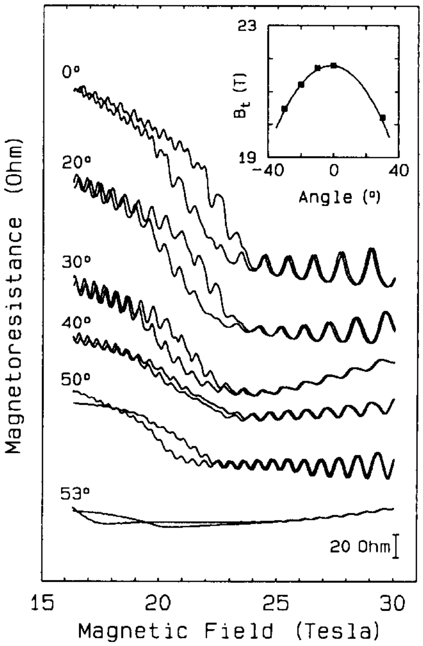

Fig. 6. Angular dependence of the high field (MR) showing a drop ("kink") in resistance around 22 T; the traces are offset for clarity and the temperature is 490 mK. The inset shows the angular dependence of the "kink" (points) fitted to a $\cos^{1/2}\theta$ dependence (line).

these oscillations reveals that the product of the effective mass and the g-factor, m^*g^*, is 4.02 ± 0.02. (Note that the SdHo frequencies below the transition also follow a $1/\cos\theta$ dependence, but the dependence of their amplitudes on tilt angle is somewhat different, indicating that $m^*g^* = 3.07 \pm 0.02$ [7] for the $F1$ series. The angular dependence of the high-field resistive transition has also been measured and is found to have the approximate functional form $B = B_0 \cos^{1/2}\theta$, see fig. 6(c).)

It therefore appears that the behaviour of the MR above the transition is fairly "conventional". Indeed, if we compare the predicted area of the 2D pocket at the Brillouin zone corner (fig. 3(c)); calculated using the room-temperature crystal structure [8, 10]) with the SdHo frequency ($B_F = 656 \pm 10$ T) the agreement is very good. In addition, the absolute value of the MR at fixed fields above the 22 T transition shows Yamaji oscillations [6], which confirms this interpretation and which indicates that the 2D pockets are roughly circular. Therefore we can say that above the 22 T transition the experimental MR is in agreement with the band structure calculation whereas the situation is rather more complicated at lower fields.

$ET_2KHg(SCN)_4$ is known to be in an antiferromagnetic ground state below ~10 K [8], and the internal magnetic order obviously plays some part in the high-field transition, and the observation of two SdHo frequencies and hysteresis below it. As a first attempt to explain these phenomena, we propose that the system is not only antiferromagnetically ordered within the plane (perhaps due to an incommensurate spin-density wave associated with the quasi-one-dimensional part of the Fermi surface), but that there is also a magnetic superlattice in the ***b*** direction, causing a doubling of the unit cell along this axis. A possible mechanism for this is canted antiferromagnetic order within each plane, with the direction of the canted moment alternating from one layer to another. This will fold back the Fermi surface in the ***b*** direction, leading to the situation in fig. 3(d): the Fermi surface now consists of four open sections and two concentric 2D closed orbits at the zone corners, leading to two series of SdHo of similar frequencies. The non-Dingle field dependence of the SdH amplitude of $F2$ could signal magnetic depopulation of one of these pockets of carriers. This will affect only the phase, and not the frequency, of the SdHo provided the change in areal carrier density per pocket is approximately linear in B [11]; this is the natural dependence in a 2D system when the energy shifts are linear in B. At high fields, the external field may overcome the weak inter-plane antiferromagnetic ordering, creating a canted antiferromagnetic arrangement within the planes. This would remove the folding in the ***b*** direction, and lower the number of states available for small-***k*** scattering at the Fermi surface, thus reducing the resistance. We therefore identify this change in order with the "kink" transition occurring at around 22 T.

The varying degree of internal magnetic order between samples will lead to different splittings between $F1$ and $F2$, and the hysteresis in resistance will occur because on the downsweep, the spin system will be more ordered, leading to less spin-disorder scattering [12]; it is noticeable that the lower resistance is almost invariably seen on the downsweep, supporting this mechanism.

In summary, we have used high-field MR measurements at a variety of temperatures and orientations to study the band structure of $ET_2KHg(SCN)_4$ and $\beta''ET_2AuBr_2$. It was found that the various SdHo frequencies in $\beta''ET_2AuBr_2$ could be related to the sums and differences of two primary frequencies and their harmonics. By proposing that the band structure is altered by a 2***c*** spin density wave (SDW) modulation, we have been able to account for all of the observed MR data qualitatively. In $ET_2KHg(SCN)_4$ we have observed at low fields two dominant SdHo series, one of which is sample dependent, also having an anomalous field-dependent amplitude. Above a resistive "kink" transition at ~22 T the dominant oscillation for B perpendicular to the highly conducting layers has a fundamental field $B_F = 656 \pm 10$ T, and the band structure is similar to that calculated using the room-temperature crystal structure. We have proposed that these effects result from a magnetic superlattice in the ***b*** direction; the weak inter-plane reactions responsible for this are overcome by the external magnetic field at ~22 T, resulting in the "kink" and the simpler high-field behaviour.

Acknowledgements

This work is supported by the Science and Engineering Research Council in the UK, by Stichting voor Fundamenteel Onderzoek der Materie (FOM) in the Netherlands, and by the European Community Large Installations Plan.

References

[1] ET is BEDT-TTF or bis(ethylenedithio)-tetrathiafulvalene. For a review, see, e.g. Synth. Metals 42 (1991) 1963.

[2] F.L. Pratt, A.J. Fisher, W. Hayes, J. Singleton,

S.J.R.M. Spermon, M. Kurmoo and P. Day, Phys. Rev. Lett. 61 (1988) 2721.
[3] M. Kurmoo, D.R. Talham, P. Day, I.D. Parker, R.H. Friend, A.M. Stringer and J.A.K. Howard, Solid State Commun. 61 (1987) 459.
[4] M. Doporto, J. Singleton, F.L. Pratt, T.J.B.M. Janssen, J.A.A.J. Perenboom, M. Kurmoo, W. Hayes and P. Day, Physica B 177 (1992) 348 (these Proceedings).
[5] T. Mori, F. Sakai, G. Saitoh and H. Inokuchi, Chem. Lett. (1986) 1037.
[6] K. Yamaji, J. Phys. Soc. Jpn. 58 (1989) 1520.
[7] M. Kurmoo, unpublished results.
[8] T. Sasaki, N. Toyota, M. Tokumoto, N. Kinoshita and H. Anzai, Solid State Commun. 75 (1990).
T. Sasaki, H. Sato and N. Toyota, Synth. Metals 42 (1991) 2211.
T. Osada, R. Yagi, A. Kawasumi, S. Kagushima, N. Miura, M. Oshima, H. Mori, T. Nakamura and G. Saitoh, Synth. Metals 42 (1991) 2171.
[9] J. Wosnitza, G.W. Crabtree, H.H. Wang, K.D. Carlson, M.D. Vashon and J.M. Williams, Phys. Rev. Lett. 67 (1991) 263.
[10] H. Mori, S. Tanaka, M. Oshima, G. Saito, T. Mori, Y. Maruyama and H. Inokuchi, Bull. Chem. Soc. Jpn. 63 (1990) 2183.
[11] J. Singleton, R.J. Nicholas, F. Nasir and C.K. Sarkar, J. Phys. 19 (1986) 35.
[12] Y. Shapira, S. Foner, N.F. Oliveira and T.B. Reed, Phys. Rev. B 10 (1974) 4765.